D.C. Electric Fields in the Magnetosphere

by

Mavis Gail Cauffman

A critical essay submitted in partial fulfillment of the requirements for the degree of Master of Science in the Department of Physics and Astronomy in the Graduate College of the University of Iowa

June 1969

Chairman: Dr. Donald Gurnett

ACKNOWLEDGMENT

I would like to thank Professor Donald Gurnett for suggesting this topic and for his interest, advice, and encouragement in the preparation of this essay.

TABLE OF CONTENTS

I. INTRODUCTION

Historically, two stages in the development of magnetospheric electric field theory can be distinguished on the basis of whether or not electric fields were assumed to exist parallel to geomagnetic field lines. In the early stage it was assumed that $E_{\parallel}$ was zero, because it was believed that the unrestricted motion of plasma along magnetic field lines would quickly short-circuit any charge separations which might temporarily create electric fields. The conductivity parallel to the magnetic field, $\sigma_{\parallel}$, was thus considered to be infinite, causing the magnetic field lines to be equipotentials. Under this set of assumptions, which was often applied together with the familiar plasma physics approximation of "frozen-in" magnetic field lines, the magnetic field was thought to characterize the magnetosphere and only $\vec{v}\times\vec{B}$ electric fields due to plasma motion could be present. These assumptions were particularly convenient because it is very difficult to measure the relatively weak magnetospheric electric fields experimentally. Furthermore, most theories are considerably simplified if $E_{\parallel}$ can be ignored. Experimentally, therefore, efforts were directed towards accumulation of magnetic field data. As a result, the basic magnetic field structure and behavior is now fairly well understood and agreed upon.

More recently it has been realized that the $E_{\parallel} = 0$ assumption is true only under very special conditions, so that

in general $E_{\parallel} \neq 0$ in the magnetosphere. The relevant plasma physics is considerably more complicated for a situation in which field lines have been "thawed" due to a finite conductivity. It is now generally agreed that the electric field, in addition to the magnetic field, must be mapped before we can fully understand magnetospheric phenomena and conditions.

In this paper a cursory account will be given of the theories concerned with electric fields in the magnetosphere and of several techniques which have been used or proposed to measure them.

II. THEORY

Magnetospheric Sources and Models

There are several mechanisms by which electric fields may be generated in the magnetosphere. Theorists do not agree on their relative importance.

The entire magnetosphere is immersed in an electric field due to the motion of the solar wind. This electric field is a $\vec{v}x\vec{B}$ field due to radial motion of the solar wind plasma and its associated magnetic field [Alfven and Falthammar, 1963]. In the outer magnetosphere the strength of this electric field is estimated to be on the order of 1mV/m [Bostrom and Falthammar, 1967].

According to Axford and Hines [1961] the solar wind drags plasma in the outer magnetosphere back toward the tail. Some geomagnetic field lines are frozen into this plasma and if the magnetic field lines remain connected, there will be a buildup of plasma in the tail. A compensating return flow of plasma must result if steady state conditions are to hold. The motion of the returning plasma through the magnetosphere is thought to induce an electric field.

In the model due to Dungey[1961], merging of magnetic field lines in the solar wind with those in the magnetosphere leads to convection of plasma and resulting electric fields.

A similar flow of currents is predicted by Fejer [1961]. He suggests that temporary disturbances of radiation belt particles result in equatorial drifts of particles to reestablish equilibrium.

The Ionospheric Dynamo

Within the ionosphere itself a major mechanism exists for producing electric fields. Winds in the upper atmosphere due to solar heating cause motion of plasma relative to magnetic field lines, producing a dynamo electric field perpendicular to $\vec{v}$ and $\vec{B}$ [Sugiura and Heppner, 1968]. This dynamo field drives a current in the ionosphere. The entire closed current system is thought to lie in the ionosphere. Any particular current loop resembles a generator circuit (Figure 1). Within the generator the current is antiparallel to the electric field, whereas in the external closing loop the current is parallel to the electric field.

For an ideal upper atmospheric wind system undergoing a diurnal variation due to the diurnal solar heating effects, a current system can be derived which is consistent with the Sq magnetic variations observed on the earth [Sugiura and Heppner, 1968].The corresponding electric fields should be on the order of 1 to 5 mV/m [Bostrom and Falthammar, 1967]. The equatorial electrojet is part of this current system (Figure 2).

Justification for Non-Zero $E_{\parallel}$

The theories mentioned above assume the frozen-in condition $\vec{E} + \vec{v}\times\vec{B} = 0$, which is valid only when $E_{\parallel} = 0$ or curl $E_{\parallel} = 0$ [Falthammar, 1965]. However, observations of auroral protons indicate that some acceleration mechanism along field lines is active [Johansen and Omholt, 1963]. Further, O'Brien and Taylor [1964] suggest that parallel electric fields might explain their observations of splashes of precipitating particles.

Such observational evidence has led to serious theoretical reconsideration of parallel electric fields. Alfven and Falthammar [1963] were first to suggest that in a mirror field where the mean free path is very long an $E_{\parallel}$ can result if the pitch-angle distributions of ions and electrons are different. In the outer magnetosphere particles have very long mean free paths. That is, the effect of collisions is negligible. In the mirror magnetic field of the earth $\lambda_D << l << \lambda$, where λ_D is the Debye length, l is the length of the flux tube, and λ is the mean free path of the charged particles. A very small Debye length leads to the requirement of quasi charge neutrality [Block, 1967].

There are two ways that the condition of charge neutrality can be satisfied. The first is for $E_{\parallel}$ to equal zero, and Persson [1963, 1966] has shown that a necessary condition for $E_{\parallel}$ to vanish is that the pitch-angle distributions of ions and electrons be the same. Then an equal number of ions and

electrons are mirrored at corresponding heights and charge neutrality is maintained. If the distributions are not the same and an $E_{\parallel}$ exists, charge neutrality can still be maintained. If the $E_{\parallel}$ field is such as to contain the species of particle with smaller average pitch-angle, it will merely lower the mirror point of the particles of opposite sign. The situation is a stable one. A net current will not flow to cancel the field because the particle motions along the flux tubes are essentially random in phase. The velocity distributions and the condition of charge neutrality will determine the magnitude of the electric field.

If the pitch-angle distributions are not identical, then one of them, at least, must be anisotropic, leading to instabilities. Block [1967] discusses such instabilities and the precipitation of particles which results. Comparing his results with experimental measurements, he concludes that there are fairly static $E_{\parallel}$ fields present in the ionosphere which are sporadically cancelled by instabilities.

Coupling Between the Magnetosphere and the Ionosphere

Any large-scale transverse electric field in the magnetosphere should to some degree affect the electric field in the ionosphere. At first, assuming an essentially infinite parallel conductivity, it was thought that the electric field simply mapped down the (equipotential) magnetic field lines. The strength of the electric field at ionospheric heights due to the electric field caused by the solar wind motion would then be 100 mV/m [Bostrom and Falthammar, 1967]. However, it has recently been estimated that potentials of up to 10kV can exist along magnetic field lines [Bostrom and Falthammar, 1967] and may be different along different field lines. Assuming an ionospheric transverse field of 100 mV/m, electric fields with dimensions of less than

$$10\text{kV} / (100\text{mV/m}) = 100\ \text{km}$$

at E layer altitudes need not be related to magnetospheric electric fields [Bostrom, 1967].

Equivalence of Currents and Electric Fields

Magnetospheric current systems and electric field patterns must be consistent. If either the electric field or the current is known, the other will be given by

$$\vec{I} = \sigma_P \left(\vec{E}_\perp + \vec{v}_n \times \vec{B} \right) + \sigma_H \frac{\vec{B} \times (\vec{E}_\perp + \vec{v}_n \times \vec{B})}{B} + \sigma_{\parallel} \vec{E}_{\parallel}$$

where $\vec{v}_n$ = neutral gas velocity

σ_P = Pedersen conductivity

σ_H = Hall conductivity

$\sigma_{\parallel}$ = conductivity parallel to the magnetic field

if the conductivities are known, or can be measured [Bostrom and Falthammar, 1967]. It is apparent from this equation that the current does not always flow parallel to the electric field. Since the relative magnitudes of the various conductivities change with altitude, the relation between the directions of the current and the electric field will also vary.

The DS current system is derived from ground-based magnetic disturbance measurements (S_D) mainly in the polar region on the assumption that the causative currents are confined to a shell in the ionosphere. In reality there will be currents along the magnetic field lines, but since the perpendicular conductivity is very high within a fairly thin (perhaps 10 km thick) region in the ionosphere, a shell of current is a reasonable approximation. Alfven and

Falthammar [1963] show that the main effect of the magnetic field in such a situation is to concentrate most of the current in the region of high conductivity.

The auroral electrojet is the most intense part of the DS current system. The electrojet is on the order of 10^6 amperes at a height of about 100 km [Alfven, 1967] and is directed to the west on the morning side of the earth and to the east on the evening side (Figure 3). Bostrom [1967] discusses two systems for closing the currents in the magnetosphere (Figure 4) depending upon the relative importance of the Pedersen and Hall currents in producing a disturbance of the horizontal component of the magnetic field at the earth. He calculated that an equatorial electric field of about 60 mV/m must be present to drive an electrojet of about 10^4 amperes in a 10 km thick auroral arc.

One theory proposed for driving the auroral electrojet is an asymmetrical ring current. According to Piddington [1967], if the ring current were confined mostly to the night side, a separation of charge would result with electrons on the sunrise side and ions on the sunset side. There would then be a tendency to short out this separation by a flow of current down the field lines, across the highly conducting E region of the ionosphere and back up the field lines on the other side of the earth.

Taylor and Hones [1965] derive a model electric field

pattern based on DS currents. Taylor and Hones solve the tensor equation $\vec{J} = \overleftrightarrow{\sigma} \cdot \vec{E}$, where $\vec{J}$ is the height-integrated current and $\overleftrightarrow{\sigma}$ is the height-integrated conductivity tensor, assuming magnetic field lines to be equipotentials. Predictions based on their models of electric and magnetic fields are in good agreement with observations [Hones, 1968].

Predicted Values of the Electric Field Strength

As a guide to the values of the electric field which might be expected for various regions of space, Block [1966, 1967] has compiled the table which follows.

Region in Space	E (V/m)	$E_{\parallel}$ (V/m)	$V_{satellite} \times B$ (V/m)
5 R_E in equatorial plane	10^{-4}-10^{-2}	0	10^{-3}
5 R_E above pole	10^{-4}-10^{-2}	0-10^{-6}	10^{-3}
Just above the ionosphere	10^{-2}-10^{-1}	10^{-3}-10^{-1}	10^{-1}
In solar wind	10^{-4}-10^{-2}	0	10^{-5}

III. METHODS OF MEASURING DC ELECTRIC FIELDS AND EXPERIMENTAL RESULTS

Double Probes

a. Introduction

Theoretically, the most direct method of measuring the electric field is to determine the potential difference between two points in the plasma. Assuming that the plasma is isotropic on a scale of the distance between the probes, then $E = \Delta V/d$.

In an actual experiment many complications arise. One difficulty is that the probes will not be at the plasma potential because a plasma sheath will form around them. However, if the probes are identical and if spatial gradients in the plasma are negligible, the potential drop across the sheath should be the same for both electrodes. Then the measured potential difference will be that of the plasma itself.

Numerous practical difficulties exist in measuring electric fields in space in addition to the requirement of physically and electrically identical probes. The velocity-space anisotropy of the plasma requires that the probes be symmetrically oriented with respect to the plasma flow. They must be as far as possible from the spacecraft and from each other so that screening effects are minimized. Some instrumental errors also present are those due to voltmeter current, finite probe distance, and thermal noise in the circuitry.

Another class of contaminants to a measurement arises from the physics of the situation, rather than the measuring instruments. These phenomenological errors include relative velocity of the spacecraft and plasma ($\vec{v}x\vec{B}$ electric field), photoelectric current from the probes, density, temperature and velocity gradients, and high energy particle fluxes. Since the probes are in fact never identical, sheath thickness and general Langmuir probe characteristics must sometimes be considered.

The theory of double probe systems for measuring electric fields is discussed by Fahleson [1967], Aggson [1966], Storey [1964], and others. The review here is based principally upon the treatment by Fahleson.

b. Single Probe Potential

The voltage drop between a single probe and the surrounding plasma is very difficult to calculate. It is considered at this point both in order to explain why single-probe measurements of the plasma potential are impractical and in order to justify the demand that sets of double probe antennas be identical. The equations derived will be useful in estimating the effects of errors in later sections, even though the expressions are far from exact.

The potential of an electrode isolated electrically in a plasma is determined by the various currents present.

Because the ion mass is much larger than the electron mass, the electron saturation current to a neutral probe will exceed the ion saturation current [Storey, 1964]. This drives the probe negative with respect to the plasma, and equilibrium is reached when the probe is sufficiently negative that the electron and ion currents to it are equal. In the bulk of the magnetosphere, this is the dominant mechanism among those competing to control the probe potential. In the outer magnetosphere, however, photoemission of electrons may become important enough to drive the probe positive.

The detailed interaction between an electrode immersed in a plasma and the plasma is given by Langmuir probe theory [Langmuir and Mott-Smith, 1926] and only the relevant equations will be given here. For simplicity, only the case of spherical electrodes is considered. The plasma is assumed to be Maxwellian. The first situation considered is the more common case of a negatively-biased electrode. The electron and ion currents to a spherical probe are

$$I_e = -4\pi r^2 ne \left(\frac{kT_e}{2\pi m_e}\right)^{1/2} \exp\left(eV/kT_e\right) \qquad (1)$$

$$I_i = 4\pi a^2 ne \left(\frac{kT_i}{2\pi m_i}\right)^{1/2} \left(1 - \frac{a^2-r^2}{a^2} \exp\left(-\frac{r^2}{a^2-r^2}\frac{eV}{kT_i}\right)\right)$$

where r = spherical probe radius

a = outer radius of plasma sheath

n = electron density of undisturbed plasma = ion density

e = elementary charge

k = Boltzmann's constant

m_e = electron mass

m_i = ion mass

T_e = electron temperature

T_i = ion temperature

V = probe potential with respect to the plasma for a negatively-biased spherical probe.

The potential V is to be determined.

The sheath thickness is

$$a-r = \lambda_D \, (eV/kT_e)^{1/2}$$

where

$$\lambda_D = (\varepsilon_o kT_e/ne^2)^{1/2}$$

is the Debye length and ε_o is the dielectric constant of vacuum. The potential V of the probe will be determined by current conservation. The current flowing through the lead from the probe to the voltmeter is

$$I = I_{ph} + I_i + I_e \qquad (2)$$

where I_{ph} is the current due to photoemission of electrons,

$$I_{ph} = \pi \, r^2 \, i_{ph} \, . \qquad (3)$$

In sunlight i_{ph} is typically 10^{-4} amp/m^2, but it depends on the probe material as well as the illumination and so is accurate only to within an order of magnitude. In darkness, $I_{ph} = 0$.

If the probe radius r is much longer than the sheath thickness (a-r), the ion current will be

$$I_i = \pi r^2 ne \, (8kT_i / \pi m_i)^{1/2} \tag{4}$$

However, because the probe may be moving through the plasma, the ion current may be larger than indicated by equation 4. According to Fahleson [1967]

$$I_i = \pi r^2 ne \left(\frac{8kT_i}{\pi m_i} + v^2 \right)^{1/2} \tag{5}$$

where v is the velocity of the probe. If the probe potential is small this result may be accurate to an order of magnitude. Solving equations 1, 2, 3, and 5, the probe potential is found to be

$$V = - \frac{kT_e}{e} \ln \frac{(kT_e/\pi 2 m_e)^{1/2}}{\left(\frac{kT_i}{2\pi m_i} + \frac{v^2}{16} \right)^{1/2} + \frac{i_{ph}}{4ne} - \frac{I}{4\pi r^2 ne}} \tag{6}$$

In sunlight at very low and very high altitudes the photoemission of electrons may dominate over the electron current from the plasma to make the equilibrium probe potential positive. The approximate probe potential can be calculated as before, neglecting the ion current, using the electron current

$$I_e = -4\pi r^2 ne \, (kT_e / 2\pi m_e)^{1/2} \tag{7}$$

and the photocurrent

$$I_{ph} = \pi r^2 i_{ph} \exp (-eV/kT_{ph}) \tag{8}$$

in equation 2. Solving equations 2, 7, and 8 with $I_i = 0$ yields

$$V_+ = \frac{-kT_{ph}}{e} \ln \left[\frac{I}{\pi r^2 i_{ph}} + \frac{4ne}{i_{ph}} \left(\frac{kT_e}{2\pi m_e} \right)^{1/2} \right] \tag{9}$$

for the probe potential with respect to the plasma of a positively-biased spherical probe. In the sections which follow, the analyses which are carried out using equation 6 for negatively-biased spheres are applicable to positively-biased spheres if equation 9 is used.

From the discussion so far it is apparent that the actual probe potential may deviate by orders of magnitude from the value given by relations 6 and 9 above. Unfortunately, a more accurate theoretical treatment is quite difficult, involving numerical integrations. Even so, it is impossible to calculate exactly the potential difference between the plasma and the probe. However, if the electric field is to be determined from the potential difference between two probes such as spheres for which equations 6 and 9 were derived, an accurate result can nevertheless be obtained if both probes are identical.

In the sections which follow, factors which cause deviations from this ideal situation are discussed.

c. Contact Potential

The contact potential is the potential between spheres due to their electrical and physical differences. This causes a small constant voltage difference between the probes. Often it can be eliminated by averaging the readings from a spinning probe system and subtracting the constant component. Effects as ordinary as a fingerprint on one sphere can, by changing the electron photoemission current, significantly affect the contact potential. With precautions, however, the errors can be kept below a millivolt [Aggson, 1966].

d. Voltmeter Current

Two spherical probes connected in the manner illustrated in Figure 5 will establish themselves at a potential difference slightly less than the corresponding plasma potential difference due to the current drawn by the voltmeter between them. This current increases the potential of the most negative probe and decreases the potential of the other probe. For a small current, the voltmeter reads

$$V_M = E'd - 2\,\Delta V$$

where d is the probe separation and $\Delta V = \left|\frac{\partial V}{\partial I} I\right|$ is the change in a probe's potential due to the current. The dynamic impedance $\frac{\partial V}{\partial I}$ can be found from equation 6 to be

$$\frac{\partial V}{\partial I} = \frac{(2\pi m_e kT_e)^{1/2}}{4\pi r^2 ne^2} \exp(-eV/kT_e)$$

which is valid for negative V. Requiring

$$|I|R \approx E'd > \frac{2\Delta V}{\alpha} = \frac{2}{\alpha} \left|I \frac{\partial V}{\partial I}\right|$$

gives

$$r^2 R\alpha = \frac{(2\pi m_e kT_e)^{1/2}}{2\pi ne^2} \exp(-eV/kT_e)$$

which relates the probe radius r, voltmeter resistance R, and fractional error α. Note that the probe potential is a parameter. Some experimenters have proposed biasing the probes using a third electrode and battery or a collimated hot filament that feeds electrons back to the plasma [Fahleson, 1967].

e. Finite Probe Distance

The radius of the sheath which forms around probes in plasmas will typically be several times the Debye length, which varies from a few millimeters in the ionosphere to 10 or 100 meters in interplanetary space. Clearly, unless the probe separation d is much greater than the Debye length λ_D, the two spheres will change the electric field around each other so that the field measured by assuming $E = \Delta V/d$ will not be the true electric field.

Other effects depending on the inter-probe distance are shading and screening. Optical shading of either sphere will

cause a large asymmetry in the photoelectric current. Knowledge of probe orientation relative to the sun can be used to identify and discard such events.

Since the mean free path of particles generally is large compared to the probe dimensions, the probes (and spacecraft body and booms) will screen particles from each other. The solid angle subtended by the screening object as seen by a probe can be made negligibly small by increasing d relative to the probe radius r. Screening by the booms may be important when $r \cong \lambda_D$. One way to minimize this effect is to have dummy insulated booms extend several sphere radii beyond the spheres, opposite the main booms. For most orientations of the spacecraft this eliminates the asymmetry. This discussion has assumed that the current distributions are isotropic. When the anisotropy of the medium is taken into account, larger "wake" effects can occur at certain orientations of the spacecraft.

f. Wake Effects

A spacecraft in the magnetosphere exhibits two types of wake phenomena. The first is the wake opposite the vehicle's direction of motion, or "velocity wake". Because charged particles are constrained to helical paths about geomagnetic field lines, the spacecraft also has a "magnetic wake" along the magnetic field lines it intersects. This is in general a bi-directional wake.

Making the reasonable assumption that the thermal ion velocity is less than the satellite velocity, which in turn is much less than the average electron velocity, the principal feature of the velocity wake will be that the ions have been swept out of it by the spacecraft or probe. The electrons, by comparison, will not be greatly affected [Storey, 1964]. The probe thereby becomes more positive in a way which depends on velocity, in agreement with equations 5 and 6.

When one probe enters the velocity wake of the other probe or of the spacecraft, extremely large asymmetries in the ion currents to the two probes will result, producing anomalously great measurements of the sphere potential difference. These contaminants to the data can be recognized and discarded. The effect of the velocity wakes of the booms is harder to recognize.

In order to consider the effects of the magnetic wake it is assumed that the average ion gyroradius is much larger than the probe radius, which in turn exceeds the gyroradius of the thermal electrons. Under these circumstances, which are generally applicable to the magnetosphere, the ion collection by a sphere would be very little different than if there were no magnetic field. However, the electrons collected by a sphere would be those with guiding centers on or very near the field lines intersecting the sphere. Hence the sphere screens electrons from its magnetic wake. If

more electrons are travelling in one direction than the other along the field line, noticeable effects might result when one sphere enters the magnetic wake of the other, or of the spacecraft.

g. Thermal Noise

The resistance R between the probes produces a noise voltage in a bandwidth A given by

$$V_N = (4kTAR)^{1/2}$$

where T is the resistor temperature. Requiring that the noise potential is a certain fraction α of the probe potential difference gives the relation

$$E'd\alpha = (4kTAR)^{1/2}$$

which is a constraint on the probe spacing d and the resistance R.

If the potential drop across the sheaths surrounding the electrodes is small in comparison with the voltage across R, thermal noise from the sheaths will be negligible.

h. $\vec{v}x\vec{B}$ Fields

The largest phenomenological contaminant to an electric field measurement by a spacecraft arises from the motion of the spacecraft across magnetic field lines. If there exists a magnetic field $\vec{B}$ and an electric field $\vec{E}$ in a given reference frame, the electric field $\vec{E}'$ measured in a reference frame

moving with nonrelativistic velocity $\vec{v}$ with respect to the first is

$$\vec{E}' = \vec{E} + \vec{v}x\vec{B} \quad .$$

Thus the electric field in the reference frame of the earth, which is of physical interest, is

$$\vec{E} = \vec{E}' - \vec{v}x\vec{B}$$

where $\vec{E}'$ is the electric field measured by a satellite or rocket, $\vec{v}$ is the spacecraft velocity, and $\vec{B}$ is the geomagnetic field. Clearly, for a precise determination of $\vec{E}$, all three quantities $\vec{v}$, $\vec{E}'$, and $\vec{B}$ must be precisely known. This argument applies regardless of the type of electric field measuring device the spacecraft carries.

i. Velocity Gradients

The potential of a probe depends upon its velocity through the ion current I_i. If there are velocity gradients in the plasma or if the set of probes rotates, each probe will have a different velocity with respect to the plasma. The potential difference between two spheres due to a maximum angular velocity difference $\Delta\omega$ will be, to first order,

$$\Delta V_\omega \cong \Delta\omega \frac{\partial V}{\partial v}$$

From equation 6 it is found that

$$\frac{\partial V}{\partial v} = \frac{v}{16e}\left[\frac{2\pi m_e kT_e}{\frac{kT_i}{2m_i} + \frac{v^2}{16}}\right]^{1/2} \exp(-eV/kT_e)$$

The potential difference due to a maximum velocity gradient Δv between spheres will be

$$\Delta V_v \cong \Delta v \frac{\partial V}{\partial v}$$

The principal way to minimize ΔV_v is to bias the probe near the plasma potential so that the ion current, which causes this error, is small compared to the electron current.

j. Density and Temperature Gradients

Just as for the case of velocity gradients, the first-order effect ΔV on the sphere potential is $\Delta V_n = \Delta n \frac{\partial V}{\partial n}$ for a density gradient with variation Δn between spheres, and $\Delta V_T = \Delta T_e \frac{\partial V}{\partial T_e}$ for a temperature gradient with variation ΔT_e between spheres. For V negative,

$$\frac{\partial V}{\partial n} \approx -\frac{kT_e}{ne} \qquad \frac{\partial V}{\partial T_e} \approx \frac{V}{T_e} - \frac{k}{2e}$$

These errors can in some cases be restrictive. Fahleson [1967] suggests that rapid variation of the bias voltage of the probe system can in principle separate the effects.

Probes become charged negatively by friction against neutral gas [Medved, 1965]. Thus for low altitude probes, density variations in the neutral gas may produce a non-negligible effect on the voltage measurement.

k. High Energy Particle Fluxes

A homogeneous flux of high energy particles may change the floating potential of a system of probes. This effect is important only above calculable critical flux levels. For moderate fluxes, even though the floating potential may be affected, no error is introduced in the voltage difference measured by the probes.

If the particle flux is inhomogeneous, however, an error is introduced in the potential measured. This error can be calculated to first order as in the preceding paragraphs, with

$$\Delta V_{\phi_j} = \Delta\phi_j \frac{\partial V}{\partial \phi_j}$$

where j denotes species, for a maximum inhomogeneity $\Delta\phi_j$.

1. Experimental Results From Rocket- and Satellite-Borne Probe Systems

The data from one rocket launched near midnight at Andenes, Norway during auroral activity is discussed by Mozer and Fahleson [1968]. In this experiment four spherical probes were mounted to form a rectangle in a plane containing the rocket spin axis. The rectangle was oriented with two sides parallel and two sides perpendicular to the rocket spin axis. Perpendicular electric fields of between 10 and 60mV/m in a southward direction were measured. During part of the

flight the data implied the existence of a 20 mV/m parallel electric field.

On several occasions the rocket passed through auroral arcs. At the boundaries of an arc temporary large scale oscillations of the perpendicular component of the electric field were detected. The perpendicular electric field was of the same order of magnitude inside and outside the arc.

The electric field experiment on Injun 5 consists of a single double-probe antenna oriented perpendicular to the magnetic field. A preliminary investigation of the probe data indicates that ionospheric perpendicular electric fields of approximately 30 mV/m may be present in the auroral zones [Gurnett et al., 1969].

m. Experimental Results From a Balloon-Borne Probe System

In addition to being flown on rockets and satellites, probe systems have been carried into the upper atmosphere by balloons. Mozer and Serlin [1969] report launching two balloons, each carrying three mutually orthogonal pairs of spherical probes, from Ft. Churchill, Canada in August of 1968.

Since a balloon essentially corotates with the earth, the $\vec{v}x\vec{B}$ contamination is negligible. Also, wake and other velocity-dependent effects will be much smaller than in rocket or satellite experiments.

In the upper atmosphere there are vertical electric fields associated with low altitude weather phenomena and horizontal electric fields which Mozer and Serlin claim are of ionospheric origin. Mozer and Serlin assume that the atmosphere has an ionospheric electric field impressed upon it at an altitude of approximately 100 km and weather-associated electric fields impressed upon it at a lower boundary. Treating the conductivity as a scalar quantity varying only with altitude, the electric field as a function of altitude is determined by solving the boundary value problem. Mozer and Serlin conclude that horizontal electric fields in the upper atmosphere are averages over distances of a few hundred kilometers and over times of approximately one second of the horizontal ionospheric electric field.

Equatorial horizontal electric fields during magnetically quiet and active periods were measured to be 0.6mV/m and 1.0 mV/m, respectively.

Barium Clouds

In 1962 a group at the Max Planck Institute near Munich began work on another method of measuring electric fields. By generating artificial plasma clouds in the upper atmosphere and observing their motions, a determination of the electric field necessary to cause the measured drifts can be made. The clouds are generated by releasing from rockets a substance which will be ionized by solar radiation. The release must occur at twilight so that the sun-lit cloud will appear against a dark background.

The material to be used must have the following properties [Haerendel and Lust, 1968b]:

(1) Neutral atoms must have a high probability of being ionized by solar ultraviolet radiation.

(2) Resonance lines of the ions must lie in the optical range so that the emitted light can penetrate the atmosphere and be observed.

(3) The excitation probability of these lines must be high.

Elements having these properties are Ba, Sr, Eu, and Yb. Strontium was the first element used, but no ionization was observed. Barium proved to be more suitable. Within 10 seconds after release an ionized cloud can be seen.

The ionized and non-ionized clouds can be distinguished by differences in color and shape. Non-ionized barium emits green light, ionized barium emits purple, and neutral strontium,

which is always an impurity in barium, emits blue [Haerendel and Lust, 1968a and b]. Since the strontium does not become ionized, its motion leads to a determination of the neutral wind velocity. The non-ionized cloud remains roughly spherical, expanding at a decreasing rate as collisions with atmospheric particles become more and more effective in slowing the neutral particles. The ionized cloud is constrained to expand along magnetic field lines, and so takes on a cylindrical shape. Figure 6 schematically depicts the behavior of the neutral and ionized clouds as a function of time.

The motion of the elongated ion cloud perpendicular to the magnetic field is due to the influence of the perpendicular component of the electric field. Triangulation on the visual center of the cloud yields a measurement of the perpendicular velocity, but as time passes and the cloud diffuses there is much more scatter in the data. Haerendel et al. [1967] have derived an expression for the perpendicular component of the electric field,

$$\vec{E}_\perp = \frac{1 + \lambda^*}{2} B \left(\frac{\vec{B}}{B} \times \vec{v}_\perp + \frac{1}{k_i} (\vec{v}_\perp - \vec{v}_{n\perp}) + \frac{\lambda^* - 1}{\lambda^* + 1} \vec{V}_n \times \frac{\vec{B}}{B} \right) \quad (10)$$

where λ^* is the ratio of the integrated Pedersen conductivities along the field lines intersecting the cloud and outside the cloud, $\vec{V}_n$ is the transverse neutral wind velocity, and k_i is the ratio of barium-ion gyro frequency to the frequency of

collisions between barium ions and neutrals. The rocket releasing the barium can measure the electron density profile during its flight and this data will yield the height-integrated Pedersen conductivities.

If the cloud is released at a high enough altitude, k_i is large and the second term will be small. At 200 km k_i is approximately 100. If the cloud affects the ionospheric conductivities, the third term will not be negligible. However, it has been found that the cloud does not disturb the conductivities if approximately 10 grams of material are released [Haerendel and Lust, 1968b]. In the limits of $\lambda^* = 1$ and $k_i >> 1$, equation 10 becomes

$$\vec{E} = - \vec{v} \times \vec{B}.$$

Most experiments are carried out at altitudes of about 210-240 km. These altitudes can be reached by fairly inexpensive rockets. However, in March, 1969 a barium cloud was released from HEOS-1 in an experiment directed by Lust and Gollnitz [ESRO Communique, 1969]. The altitude of release was 70,000 km and the cloud was observed from the ground, but no results have been published yet.

During five experiments at Kiruna, Sweden, perpendicular ionospheric electric fields of between 2 and 20 mV/m were measured [Haerendel and Lust, 1968b]. The electric fields were directed toward the north-west in the evening, and

toward the south-west in the morning. The fields were highly variable, but were quite well correlated with ground-based magnetometer data.

During experiments at middle magnetic latitudes, electric fields of 1-3mV/m were measured [Haerendel and Lust, 1968b]. The latter seem to support the dynamo theory of the Sq current system. The data are not complete, but it was found that at approximately 5 and 16 hours local time, the electric field was antiparallel to the Sq current. During the night hours, however, the electric field was parallel to the current.

Barium cloud releases carried out by Wescott et al. [1968] from Andøya, Norway measured much higher electric fields. Near an auroral arc a perpendicular electric field of 130 mV/m was measured. The authors claim that the electric field becomes smaller inside an arc, where the conductivity is high. This result is in contrast with the measurements of Mozer and Fahleson with a probe system, which indicate no difference in the perpendicular electric fields inside and outside arcs. Observations that barium clouds move parallel to auroral arcs, that is, parallel to the electrojet currents, imply that the electric field is perpendicular to currents. This indicates that the electrojets consist mostly of Hall current (Cf. Figure 4) [Wescott et al., 1968].

Striations aligned with the magnetic field were sometimes observed in the clouds. Wescott et al. [1968] found that

these striations were often quite similar in structure to that of nearby rayed auroral forms.

Electric Field Mills

Another method of measuring electric fields is the use of a "field mill". In a simple a.c. field mill, a fixed conductor (stator) is grounded through a high impedance and is regularly exposed to and shielded from the electric field by some sort of rotor. Charge is induced on the stator while it is exposed to the field, and when the stator is shielded this charge drains through the impedance. The result is an alternating voltage whose amplitude is proportional to the electric field strength.

This proportionality can be seen from the following calculation [Mapleson and Whitlock, 1955]. If

C = capacitance between stator and ground

R = resistance between stator and ground

E = electric field strength

ω = rotor frequency

and we consider a rotor such that the area exposed at time t is $a = \frac{1}{2} A(1 + \sin\omega t)$ where A is the maximum stator area.

$q = \epsilon_o Ea$ and $q_{max} = \epsilon_o EA = Q$

So, $q = \frac{Q}{2} (1 + \sin\omega t)$

$i = \frac{dq}{dt} = \omega\frac{Q}{2} \cos\omega t$ through C and R

$i_{max} = I = \frac{\omega Q}{2}$

$V_{max} = IZ = \frac{\omega\epsilon_o EAZ}{2}$ where $Z = \left| \frac{R/i\omega C}{R + \frac{1}{i\omega C}} \right|$

$= R (1 + \omega^2 C^2 R^2)^{-1/2}$

Therefore,

$$V_{max} = \frac{\omega \varepsilon_o EAR}{2} \left(\omega^2 C^2 R^2 + 1 \right)^{-1/2}$$

If $\omega^2 C^2 R^2 >> 1$, then

$$V_{max} = \frac{1}{2} \frac{\varepsilon_o EA}{C} \propto E$$

However, C will vary somewhat with a and in most experimental arrangements a is not truly sinusoidal. Both these effects tend to invalidate the simple proportionality derived here.

Though field mills are quite simple in theory, as with probes, serious complications arise when the device is immersed in a plasma. The appearance of a plasma sheath around the mill may significantly alter the electric field at the surface of the mill. Further, while the stator is exposed, charged particles may strike it. This added current will affect the voltage measurement

Wildman [1965] has suggested a method of separating the voltage measured into its two components, one due to the electric field and the other due to ion flux. If the voltage due to the electric field is

$$V_E = \omega \varepsilon_o \frac{EAR}{2} \cos\omega t \left(\omega^2 C^2 R^2 + 1 \right)^{-1/2}$$

then the voltage due to a current density j striking the stator is

$$V_j = \frac{jAR}{2} \sin \omega t \left(\omega^2 C^2 R^2 + 1 \right)^{-1/2}$$

Wildman considers two field mills, a and b, of equal areas A, operated at different frequencies but physically close enough to each other that $E_a=E_b$ and $j_a=j_b$. Since V_j and V_E are 90^o out of phase with each other, the total peak-to-peak voltage measured is $V_T^2 = V_E^2 + V_j^2$. Therefore,

$$V_{T_a}^2 = \alpha_a^2 E^2 + \beta_a^2 j^2$$

$$V_{T_b}^2 = \alpha_b^2 E^2 + \beta_b^2 j^2$$

if the mills are linear in their responses and the alphas and betas are the calibrated field and current sensitivities of the mills. Wildman had not yet analyzed any experimental data and no other reports could be found of field mills being flown in an attempt to measure electric fields in the ionosphere or magnetosphere.

Whistler Ducts

A large variety of radio phenomena are present in the magnetosphere. Although they are of secondary importance in energy transport, they do give a great deal of information concerning conditions in the magnetosphere and motions of plasma.

Of these phenomena, whistlers are the best understood [Cf. Helliwell, 1965]. Whistlers are electromagnetic waves in the 1-30 kHz frequency range which are caused by lightning flashes. These waves are thought to propagate along paths of enhanced or depressed magnetospheric ionization called ducts, which are aligned with the earth's magnetic field. Whistlers have a characteristic frequency-versus-time dispersion profile. The frequency of minimum delay, or nose frequency, of a whistler is related to the latitude of the field line along which it propagates and can be used to determine the equatorial radius of this field line. These electromagnetic waves are reflected at some altitude in the ionosphere, and so bounce back and forth between magnetically conjugate points. At a ground station a resulting "train" of whistler components is observed, each component obeying the dispersion relation.

In the present situation, dispersion of a whistler train results from two major causes: (1) The characteristic dispersion due to the ionization in the duct and (2) dispersion due to a change of magnetic field strength as the duct moves to

different radii. Dispersion due to motion of a duct occurs much more slowly than dispersion due to ionization. In a situation where a number of multicomponent whistler events are observed, the dispersion during a single event is due almost entirely to ionization. However, the change in frequency-versus-time characteristics between different events, of which the nose frequency is the most obvious, is due to radial motion of the duct. Choosing corresponding components from a series of successive events, the different nose frequencies give the successive equatorial radii of the duct. Events are selected for which the amplitude remains constant and the dispersion characteristics change gradually, indicating that the whistlers followed the same duct. Also, if the corresponding components from the first and last events display the same shape of dispersion curve, then the ion density in the duct has remained constant [Carpenter, 1966]. In Figure 7 the gradual rise in nose frequency and decrease in travel time indicate an inward motion of plasma. Assuming that whistlers generated at the same location follow the same duct, the motion of this duct is a measure of the $\vec{E} \times \vec{B}$ plasma drift. From this can be determined the east-west component of the electric field at a given equatorial radius.

A disadvantage of this method is that the electric field calculated represents some sort of average of the electric fields causing motions of a duct at various latitudes.

Uncertainties also arise because whistlers observed at one location may come from a 30^{o} range in longitude centered on the observation point.

Carpenter and Stone [1966] used this method to determine the electric field associated with a polar substorm occurring just after midnight on July 15, 1965. From the nose frequencies of whistler events observed during the storm, calculations were made of the corresponding equatorial radii of the paths. Inward plasma motions of approximately 700 m/sec were observed, corresponding to a westward electric field of about 0.3 mV/m at 4 earth radii on the geomagnetic equator. This electric field appeared to develop within 5 minutes and to remain for about 1 hour and 15 minutes.

Auroral Forms

Another indirect method of obtaining information about electric fields is to observe the motion of auroral forms. Auroral light is due to excitation of atmospheric gases by precipitating charged particles. Excitation of oxygen yields the green 5577 Å line, with a lifetime of approximately 0.75 second. Since the winds in the ionosphere have velocities of about 100 m/sec, the auroral light will be seen within 100 meters of the primary particles. So the motions of auroral forms are essentially the motions of primary particles, which are acted upon by electric and magnetic fields. Motion transverse to the magnetic field is due to electric fields and gradients in the magnetic field. The drift velocity of a particle perpendicular to the magnetic field is

$$\vec{U}_\perp = - \frac{\vec{B}}{eB^2} \times \left(e\vec{E} - \mu \text{ grad } \vec{B} - \mu \frac{d\vec{U}}{dt} \right)$$

[Alfven and Falthammar, 1963], where $\mu = mv_\perp^2 / 2B$ is the orbital magnetic moment and $v_\perp$ is the gyration velocity. For auroral conditions, Bostrom and Falthammar [1967] rewrite this equation in the form

$$\vec{U}_\perp = - \frac{\vec{B}}{eB^2} \times \{ e\vec{E} - \mu(1 + 2 v_\parallel^2 / v_\perp^2) \text{ grad } \vec{B} \}$$

where $v_\parallel$ is the velocity component parallel to the magnetic field. If the grad B term can be estimated, a value of the electric field is determined.

Visual aurora usually move to the west before midnight and to the east after midnight with velocities of approximately 1 km/sec. This implies the existence of electric fields in the ionosphere with strengths of approximately 50 mV/m, directed southward after midnight and northward before midnight [Bostrom, 1967]. Velocities in the north-south direction have been found to be on the order of 0.1 km/sec [Cole, 1963].

IV. CONCLUSIONS

Carefully-designed probe systems seem to promise the most accurate electric field measurements at present. The theory is fairly well understood, although complicated, and estimates can be made of most of the errors involved. If a rotating system or three orthogonal sets of probes are flown, vector determinations of the electric field can be made. By using rockets, satellites, and balloons, any region of the ionosphere or magnetosphere can be reached at any time.

Field mills operated in a plasma are still neither well understood theoretically, nor proven operationally. The other methods discussed in this paper are also limited in application. Barium clouds yield fairly direct measurements of the perpendicular component of the electric field vector, but are not particularly precise and are limited to twilight conditions. Needless to say, auroral arcs are not subject to the experimenter's control. The whistler duct method is limited to determining an average east-west component of the electric field along closed magnetic field lines.

REFERENCES

Aggson, T., "A Proposal for Tri-Axial Electric Field Measurements on IMP Spacecraft H, I, and J," NASA-GSFC, Greenbelt, Maryland (1966).

Alfven, H., "On the Importance of Electric Fields in the Magnetosphere and Interplanetary Space," Space Sci. Rev. 7, 140-148 (1967).

Alfven, H. and C.-G. Falthammar, Cosmical Electrodynamics (Clarendon Press, Oxford, England, 1963).

Axford, W. I. and C. O. Hines, "A Unifying Theory of High-Latitude Geophysical Phenomena and Geomagnetic Storms," Canadian J. Phys. 39, 1433 (1961).

Block, L. P., "On the Distribution of Electric Fields in the Magnetosphere," J. Geophys. Res. 71, 855-864 (1966).

Block, L. P., "Coupling Between the Outer Magnetosphere and the High-Latitude Ionosphere," Space Sci. Rev. 7, 198-210 (1967).

Bostrom, R., "Auroral Electric Fields," 293-303 in Aurora and Airglow, ed. by B. M. McCormac (Reinhold Book Corporation, New York, 1967).

Bostrom, R. and C.-G. Falthammar, "Scientific Background and Expected Properties of Electric Fields in the Ionosphere," in Vol. 3 of Project Study of a Rocket Payload for Electrostatic Field Measurements at High Altitudes, SAAB Electronics Labs. Rept. No. ZG-Civ-3 B43:3, Goteborg, Sweden (1967).

Carpenter, D. L., "Whistler Studies of the Plasmapause in the Magnetosphere," J. Geophys. Res. 71, 693-709 (1966).

Carpenter, D. L. and K. Stone, "Direct Detection by a Whistler Method of the Magnetospheric Electric Field Associated with a Polar Substorm," Planet. Space Sci. 15, 395-397 (1967).

Cole, K. D., "Motions of the Aurora and Radio-Aurora and their Relationships to Ionospheric Currents," Planet. Space Sci. 10, 129 (1963).

Dungey, J. W., "Interplanetary Magnetic Field and the Auroral Zones," Phys. Rev. Letters 6, 47 (1961).

ESRO Communique, Neuilly, France, No. 105, March 17 (1969).

Fahleson, U. V., "Theory for Electric Field Measurements in the Magnetosphere with Electric Probes," Space Sci. Rev. 7,238-262(1967).

Falthammar, C.-G., "Some Aspects of Particles and Fields in the Magnetosphere," 71-102 in Proceedings of a Symposium on High Latitude Particles and the Ionosphere, ed. by B. Maehlum (Logos Press, London, 1965).

Fejer, J. A., "The Effects of Energetic Trapped Particles on Magnetospheric Motions and Ionospheric Currents," Canadian J. Phys. 39, 1409 (1961).

Gurnett, D. A., G. Pfeiffer, R. Anderson, S. Mosier, and D. Cauffman, "Initial Observations of VLF Electric and Magnetic Fields with the Injun 5 Satellite," University of Iowa Research Report 69-19, 1969.

Haerendel, G. and R. Lust, "Artificial Plasma Clouds in Space," Scientific American 219, 80-92 (1968).

Haerendel, G. and R. Lust, "Electric Fields in the Upper Atmosphere," 271-285 in Earth's Particles and Fields, ed. by B. M. McCormac (Reinhold Book Corporation, New York, 1968).

Haerendel, G., R. Lust, and E. Rieger, Planet. Space Sci. 15 1 (1967).

Helliwell, R. A., Whistlers and Related Ionospheric Phenomena (Stanford University Press, Stanford, California, 1965).

Hones, E. W., Jr., "Electric Fields and Plasma Convection in the Magnetosphere," 403-416 in Earth's Particles and Fields, ed. by B. M. McCormac (Reinhold Book Corporation, New York, 1968).

Johansen, O. E. and A. Omholt, "Variations in the Doppler Profile of Hα in Aurorae," Planet. Space Sci. 11, 1223 (1963).

Langmuir, I. and H. M. Mott-Smith,"The Theory of Collectors in Gaseous Discharges," Phys. Rev. 28, (1926). (Reprinted in The Collected Works of Irving Langmuire, ed. by G. Suits, Pergamon Press, Vol. IV, 99, 1961)

Mapleson, W. W. and W. S. Whitlock, "Apparatus for the Accurate and Continuous Measurement of the Earth's Electric Field," J. Atmospheric and Terrestrial Phys. 7, 61 (1955).

Medved, D. B., "On the Formation of Satellite Electron Sheaths Resulting from Secondary Emissions and Photoemission," in Interactions of Space Vehicles with an Ionized Atmosphere, ed. by S. F. Singer (Pergamon Press, 1965).

Mozer, F. S. and U. V. Fahleson, "Parallel and Perpendicular Electric Fields in an Aurora," Space Sciences Laboratory Research Report, University of California, Berkeley (1968).

Mozer, F. S. and R. Serlin, "Magnetospheric Electric Field Measurements with Balloons," Space Sciences Laboratory Research Report, University of California, Berkeley (1969).

O'Brien, B. J. and H. Taylor, "High-Latitude Geophysical Studies with Satellite Injun 3, Part 4: Auroras and Their Excitation," J. Geophys. Res. 69, 45 (1964).

Persson, H., "Electric Field Along a Magnetic Line of Force in a Low-Density Plasma," Phys.Fluids 6, 1756 (1963).

Persson, H., "Electric Field Parallel to the Magnetic Field in a Low-Density Plasma," Phys. Fluids 9, 1090 (1966).

Piddington, J. H., "Space Electrodynamics," a series of lectures given at SUI in 1967.

Storey, L. R. O., "The Design of an Electric Dipole Antenna For VLF Reception within the Ionosphere," Centre National D'Etudes Des Telecommunications, Technical Report No. 308TC (1964).

Sugiura, M. and J. P. Heppner, "The Earth's Magnetic Field," 5-92 in Introduction to Space Science, ed. by W. N. Hess and G. D. Mead (Gordon and Breach, New York, 1968).

Taylor, H. E. and E. W. Hones, Jr., "Adiabatic Motion of Auroral Particles in a Model of the Electric and Magnetic Fields Surrounding the Earth," J. Geophys. Res. 70, 3605-3628 (1965).

Wescott, E., J. Stolarik, and J. Heppner, "Electric Fields in the Vicinity of Auroral Forms from Motions of Barium Vapor Releases,"GSFC Report No. X-612-69-62 (1969).

Wildman, P. J. L., "A Device for Measuring Electric Fields In the Presence of Ionisation," J. Atmos. Terres. Phys. 27, 417-423 (1965).

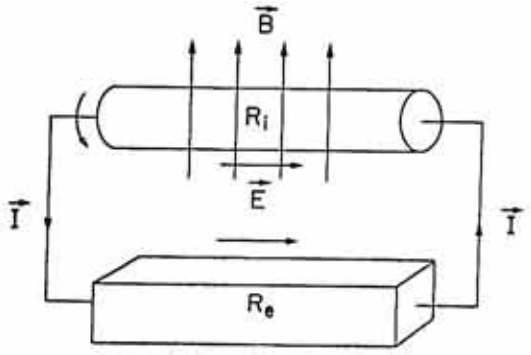

Figure 1: Equivalent Circuit for the Ionospheric Dynamo Current System (Haerendel and Lust, 1968)

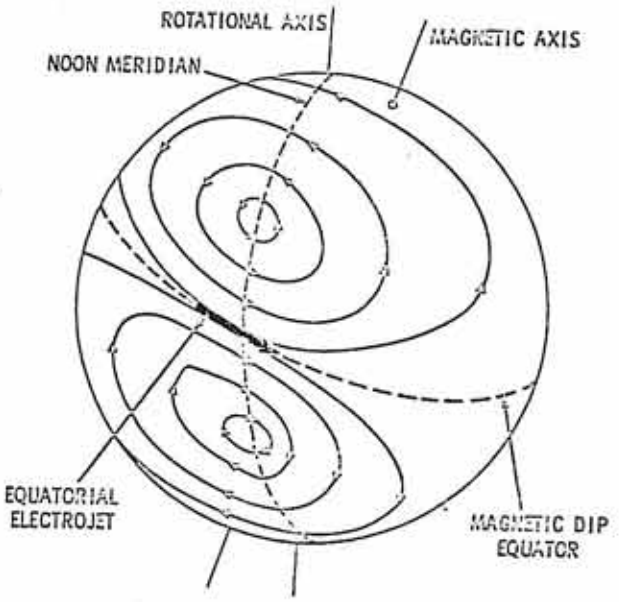

Figure 2: Sq Current System (Sugiura and Heppner, 1968)

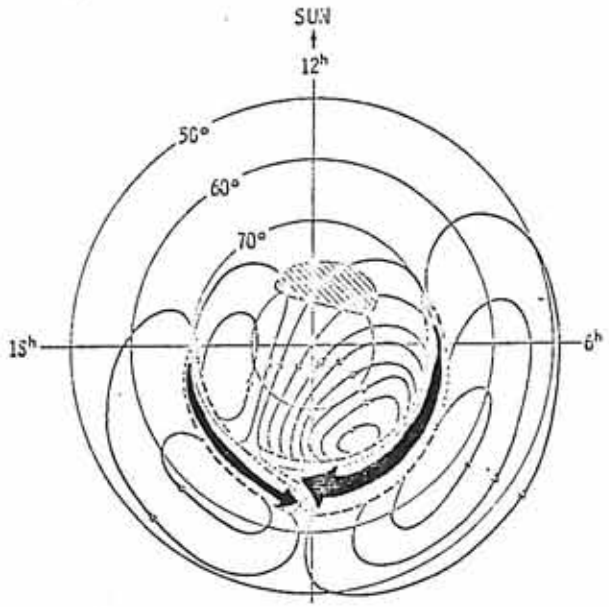

Figure 3: DS Current System (Sugiura and Heppner, 1968)

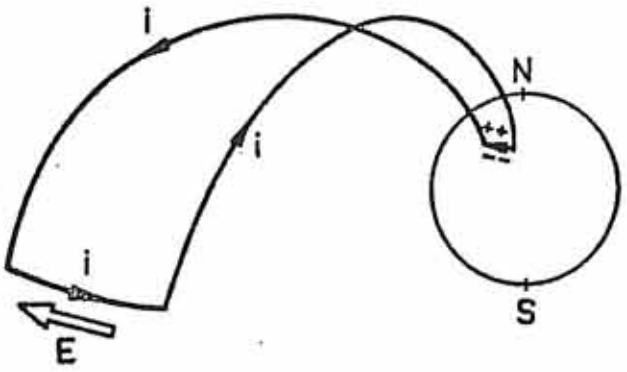

a) Both Hall and Pederson currents contribute to DS.

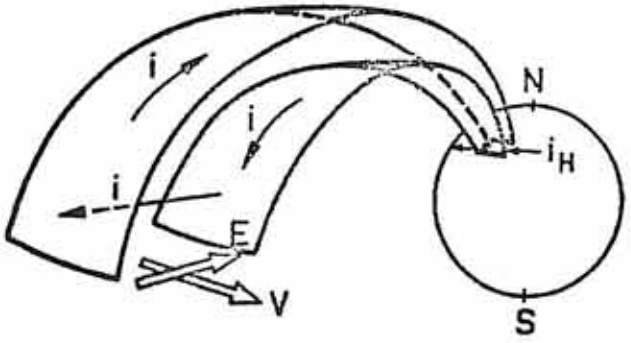

b) Only the Hall current contributes to DS.

Figure 4: Alternative models of the auroral electrojet giving the same magnetic disturbances on the ground. (Bostrom, 1967)

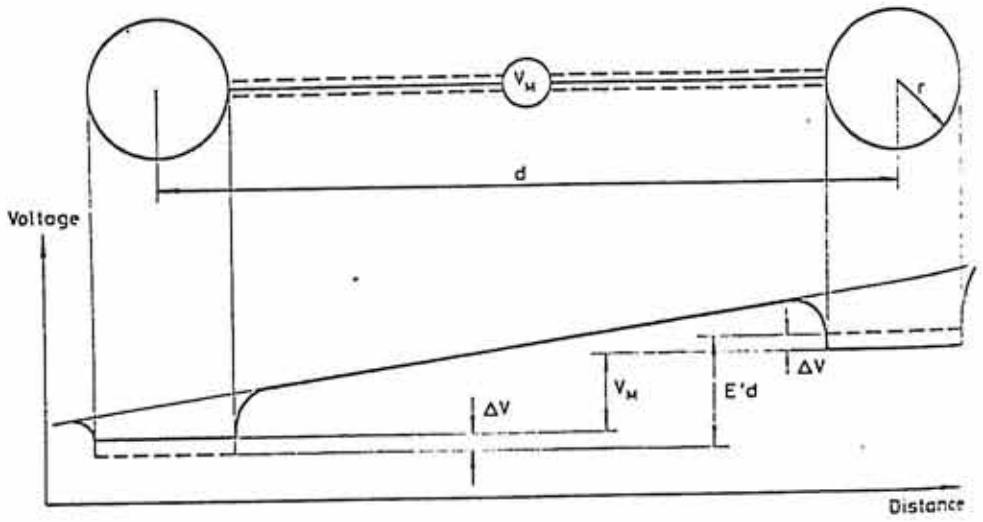

Figure 5: Two-electrode probe system. Potential along a line through the probes, but outside the boom; the potential due to the boom sheath is neglected in the figure.
(Fahleson, 1967)

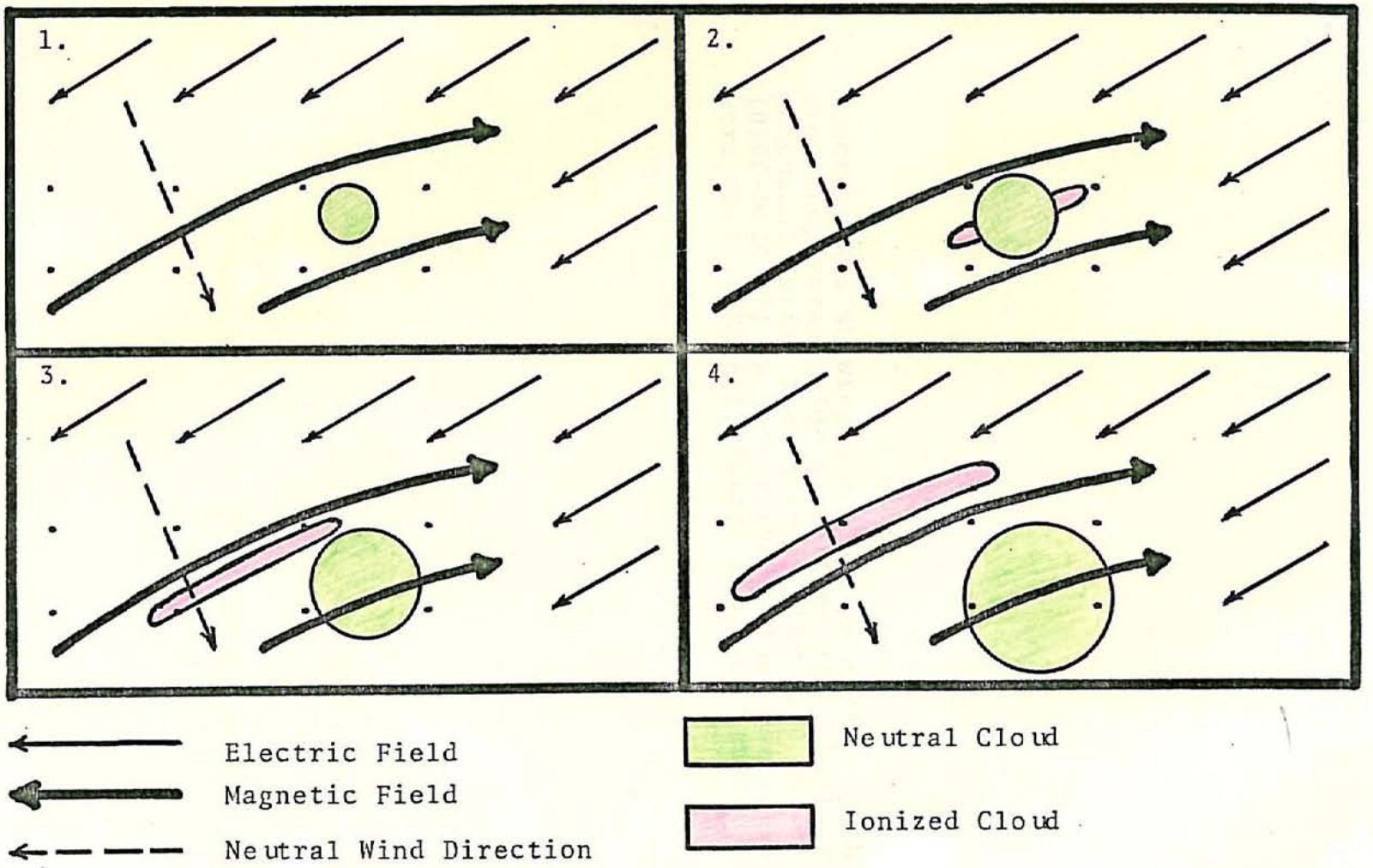

Figure 6: Schematic Development of a Barium Cloud (Haerendel and Lust, 1968a)

Figure 7: Spectrograms showing a gradual variation in the frequency-versus-time properties of a whistler component during the interval 0000-0320 LT (0500-0820 UT) on July 7,1963. The observations were made at Eights, Antarctica. (Carpenter, 1966)

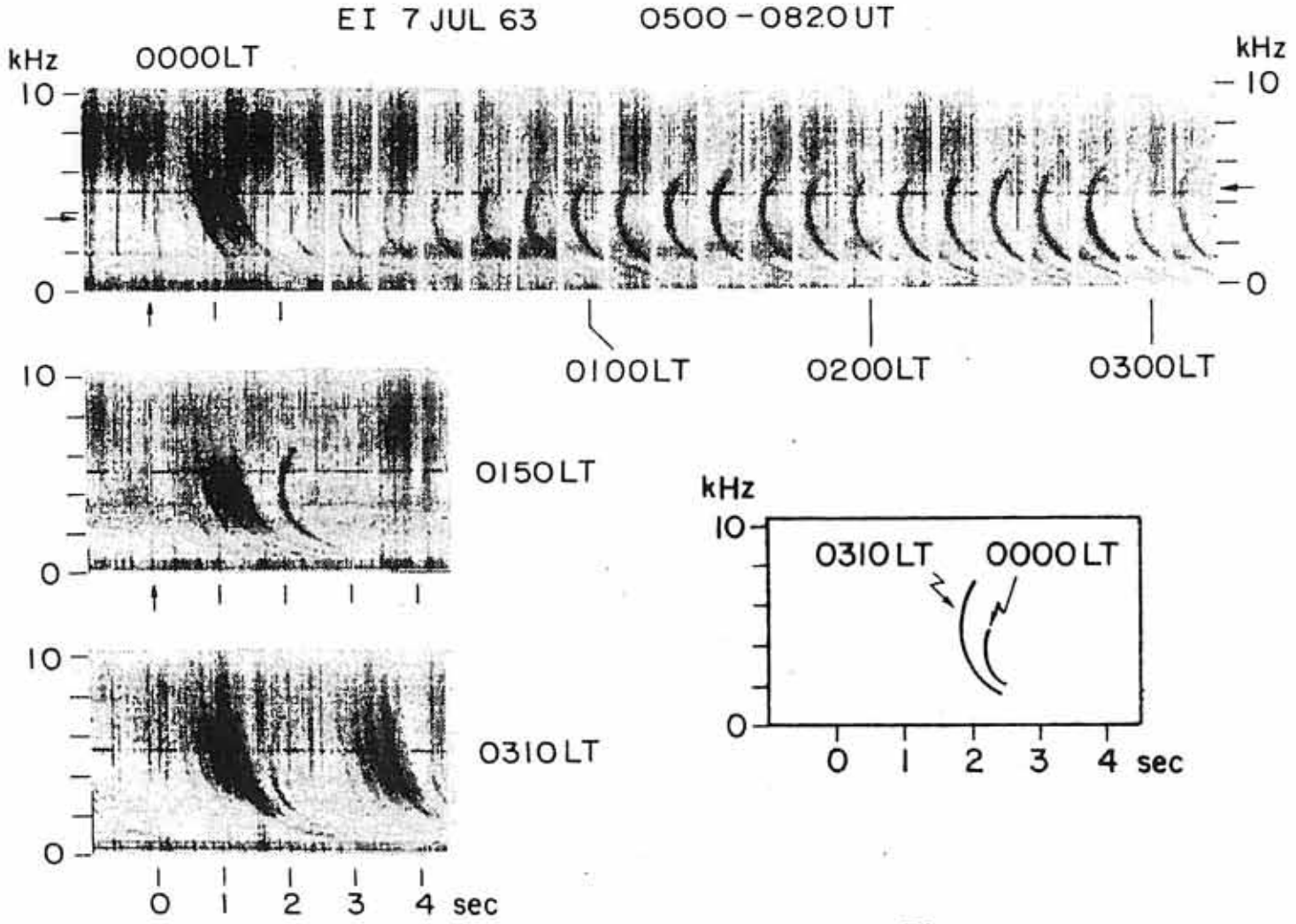
EI 7 JUL 63 0500 - 0820 UT
kHz
0000LT
10
0
kHz
10
0
0100LT
0200LT
0300LT
10
0150LT
0
10
0310LT
0
0 1 2 3 4 sec
kHz
10
0310LT
0000LT
0
0 1 2 3 4 sec

Figure 7